

ELECTROMAGNETIC ANALYSIS OF COAXIAL GYROTRON CAVITY WITH THE INNER CONDUCTOR HAVING CORRUGATIONS OF AN ARBITRARY SHAPE

G. I. Zaginaylov^{1,2,*} and I. V. Mitina¹

¹National Science Center “Kharkov Institute of Physics and Technology”, 1 Akademicheskaya St., Kharkov 61108, Ukraine

²Department of Mathematics and Mechanical Engineering, V. N. Karazin Kharkiv National University, 4 Maidan Svobody, Kharkov 61077, Ukraine

Abstract—The mathematical approach for the calculation of the membrane functions of a coaxial gyrotron cavity with an arbitrary corrugated inner rod is proposed. It is utilized mainly for two aims. First, it is shown that for typical parameters of the coaxial gyrotron cavity with the corrugated inner conductor the shape of corrugations only slightly influences the eigenvalues of competing eigen-modes. However, it can significantly influence the density of ohmic losses in the inner conductor. In particular, it is shown that the density of ohmic losses can be reduced almost twice by the proper choice of the corrugation shape. Second, it is shown that the usual idealizations of the corrugated surface of the inner conductor (the surface with rectangular grooves, having rounded edges, is approximated by a surface with wedged grooves that have sharp edges) are correct. The physical interpretation of the obtained results and their practical meaning are discussed.

1. INTRODUCTION

One of the most successful, advanced and perspective geometries for cavities of high-power gyrotrons is the coaxial cavity with the corrugated inner conductor. It can be successfully used in the ITER relevant gyrotrons of multi-megawatt output power [1]. The corrugated inner conductor plays a very important role, providing efficient mode

Received 13 May 2011, Accepted 24 June 2011, Scheduled 1 July 2011

* Corresponding author: Gennadiy Ivanovich Zaginaylov (genzag@yahoo.com).

selection, decreasing effect of beam depression, and improving the possibility of beam energy recovery and frequency tuning [2].

The basic model for the electromagnetic analysis of a coaxial gyrotron cavity is the surface impedance model (SIM) [3–5] which is used in several codes [6] for simulation of a coaxial gyrotron operation. It is rather simple and convenient for use in different simulation tools. Moreover “cold” measurements have been made to validate the correctness of this model [7]. On the basis of cold measurements of resonant frequencies and quality factors it was found that the SIM provides mostly correct results. Also there exist several other more complicated approximated models (see, for example, [8] and references therein) which have the comparable accuracy and almost the same range of applicability. However, the abovementioned measurements were made for the eigen-frequencies and parameters of the coaxial gyrotron cavity that differ from their counterparts of the last version of the coaxial gyrotron cavity [9]. Due to the restricted applicability of SIM, several more rigorous approaches have been developed [10–13]. It was found that for the typical parameters of the current versions of coaxial gyrotrons SIM yields a remarkably overestimated density of ohmic losses in the corrugated inner conductor compared to the more rigorous methods [12, 14, 15].

It should be pointed out that ohmic losses in the inner conductor are one of the most critical aspects, which should be taken into account during the design of the coaxial gyrotron cavity. The radius of the corrugated inner conductor should be chosen very carefully in order to keep the ohmic losses below a certain upper limit on one hand, and to suppress possible mode competition on the other. A comparison between the theoretical calculations and experimental results for the $TE_{31,17}$ coaxial gyrotron cavity [16] showed that the experimentally measured losses almost twice exceeded the theoretical predictions that were based on the SIM. So, compared to the rigorous full wave calculations, the measured losses are three to four times larger. The reasons for such a discrepancy are still unclear. However, it should be pointed that experiments [16] suffered from uncertainties caused by the short pulse lengths, the limited accuracy of the calorimetric measurements, and the influence of other heat sources, in particular, the dissipation of the captured stray radiation at the insert.

Nevertheless, one of the possible reasons can be associated with the idealizations of the corrugation geometry that were assumed in the rigorous full wave approaches [10–12]. In order to simplify calculations, the grooves on the surface of the inner conductor were assumed to be wedged and to have sharp edges (see Fig. 1(a)). However, in experiments the form of the grooves is rectangular, edges of the

corrugations are not infinitely sharp, and they are rounded with a certain small radius (Fig. 1(b)). Since the width and depth of the corrugations much smaller than the radius of the inner conductor, the difference between the wedge-shaped and rectangular grooves appears to be negligibly small. Nevertheless, the near-fields in close proximity of the corrugations can be noticeably different at least locally near edges. The influence of the distinctions between the idealized and realistic geometry of corrugations on the near-field and the average density of ohmic losses in the inner conductor is still an open issue. As is well known, the transverse field components near the sharp edges grow infinitely as $r^{-1/3}$, where r is the distance from the 90° edge (see, for example, [17]). Such a behavior leads to the increasing the higher harmonics. Their contribution which is accurately taken into account by full wave approaches [10–12] can be overestimated compared to the more realistic geometry with rounded edges (see, Fig. 1(b)) where the abovementioned singularity is absent.

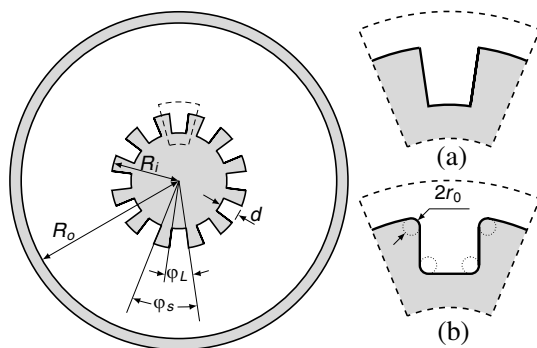


Figure 1. Typical geometry of the cross-section of a coaxial gyrotron cavity with a corrugated inner conductor; (a) wedged grooves (the sides of the grooves are directed along the radial lines) with sharp edges; (b) rectangular grooves with rounded edges.

In order to inspect the influence of these idealizations on the calculation of averaged ohmic losses in the corrugated inner conductor, a substantially new rigorous mathematical approach needs to be developed. It can be based on a modification of the boundary integral equation method [18], which was skilfully implemented numerically in [19]. As opposed to the full wave approaches [10–12], it allow us to analyze the coaxial gyrotron cavity with an arbitrarily corrugated inner conductor. Also, such an approach is useful in the study of the dependence of ohmic losses on the profile of corrugations. Such

knowledge is of practical interest because it makes possible decrease the ohmic losses in the inner conductor. One variant of such a profile is addressed below.

The rest of the paper is organized as follows. In Section 2, the new approach is described. In Section 3, one of variants of numerical implementation of the approach developed is presented. Section 4 is devoted to the inspection of the previously obtained results the idealized geometry. Also, the method of decreasing the ohmic losses in the inner conductor through proper profiling of corrugations is addressed. Conclusions are presented in Section 5.

2. FORMULATION OF THE PROBLEM AND MATHEMATICAL APPROACH TO ITS SOLUTION

The field in an arbitrary cross-section of a coaxial gyrotron cavity with a corrugated inner conductor (see, Fig. 1) is very close to the field of an infinitely long coaxial waveguide with the same cross-section.

Due to this the field of an arbitrary TE mode in a coaxial gyrotron cavity can be expressed in terms of the normalized magnetic membrane function $\psi(\vec{r}_\perp)$, which is a slow function of z [20, 21]:

$$\begin{aligned} \vec{E}_\perp &= A \operatorname{Re}\{f(z)\vec{e}(\vec{r}_\perp)e^{-i\omega t}\}, \\ \vec{H}_\perp &= A \operatorname{Re}\left\{-\frac{i}{\mu_0\omega}\vec{h}(\vec{r}_\perp)\frac{df(z)}{dz}e^{-i\omega t}\right\}, \\ H_z &= \frac{1}{i\mu_0\omega}\operatorname{rot}_z\vec{E} = A \operatorname{Re}\left\{-\frac{ik_\perp^2}{\mu_0\omega}f(z)\psi e^{-i\omega t}\right\}, \end{aligned} \quad (1)$$

where $\vec{e}(\vec{r}_\perp) = \vec{i}_z \times \nabla_\perp\psi$, $\vec{h}(\vec{r}_\perp) = -\nabla_\perp\psi$, k_\perp is the transverse wavenumber, $f(z)$ defines the longitudinal profile of the field, and A is the constant which is obtained from the balance equation (see, for example, [12, 14]).

The membrane function depends on z only through the parameters of the cross-section. It satisfies the Helmholtz equation in the region of the cross section (which is denoted as Ω) with the Neumann boundary condition at the boundary of the cross-section (denoted as Σ)

$$(\Delta_\perp + k_\perp^2)\psi = 0, \quad \vec{r}_\perp \in \Omega \quad (2)$$

$$\frac{\partial\psi}{\partial n} = 0, \quad \vec{r}_\perp \in \Sigma \quad (3)$$

where \vec{n} denotes the outer normal to the contour Σ and the variable z enters (2) and (3) as a parameter.

To get the representation for ψ , we use the second Green formula for the two-dimensional region Ω bounded by the contour Σ :

$$\int_{\Omega} (u (\Delta_{\perp} + k_{\perp}^2) w - w (\Delta_{\perp} + k_{\perp}^2) u) ds' = \int_{\Sigma} \left(u \frac{\partial}{\partial n} w - w \frac{\partial}{\partial n} u \right) dl' \quad (4)$$

Let's $u \equiv \psi$ and w is the Green function for the Helmholtz Equation (2) in the infinite two-dimensional space: $w(\vec{r}, \vec{r}') = \frac{1}{4} Y_0(k_{\perp} |\vec{r} - \vec{r}'|)$, where $Y_0(x)$ is the Neumann function of zero order. Afterwards, the index “ \perp ” in \vec{r} and \vec{r}' is omitted. Since $(\Delta + k_{\perp}^2)w(\vec{r}, \vec{r}') = \delta(\vec{r} - \vec{r}')$, when $\vec{r} \in \Omega$, the relation (4) can be reduced to

$$\psi(\vec{r}) = \frac{1}{4} \int_{\Sigma} \psi(\vec{r}') \frac{\partial}{\partial n(\vec{r}')} Y_0(k_{\perp} |\vec{r} - \vec{r}'|) dl', \quad \vec{r} \in \Omega. \quad (5)$$

The representation (5) allows us to express the magnetic membrane function ψ in the cross-section of the coaxial gyrotron cavity in terms of its value on the boundary of the cross-section. If $\vec{r} \rightarrow \Sigma$, the relation (5) becomes an integral equation. It allows us to calculate the field on Σ , and then, using (5), everywhere in the cross-section. However, when $\vec{r} \rightarrow \Sigma$ the kernel of (5) becomes singular and the relevant integral does not exist in the common sense of the term. To make (5) feasible for further consideration, let's introduce the contour Σ_{ε} , which is formed by the points $\vec{r}_{\varepsilon} = \vec{r} - \varepsilon \vec{n}(\vec{r})$, where $\vec{r} \in \Sigma$ and ε is some small parameter (see, Fig. 2). If $\vec{r}_{\varepsilon} \in \Sigma_{\varepsilon}$, then (5) is valid and the integral in (5) exists in the common sense. In order to satisfy the boundary condition (3), we take the normal derivation of (5) at the contour Σ_{ε} and then take the limit of $\varepsilon \rightarrow 0$. Finally we have:

$$\lim_{\varepsilon \rightarrow 0} \int_{\Sigma} \psi(\vec{r}') \frac{\partial}{\partial n(\vec{r}'_{\varepsilon})} \frac{\partial}{\partial n(\vec{r}')} Y_0(k_{\perp} |\vec{r}_{\varepsilon} - \vec{r}'|) dl' = 0. \quad (6)$$

If we directly put $\varepsilon = 0$ in the kernel of (6) it becomes strongly singular and non-integrable in the common sense of the term. But

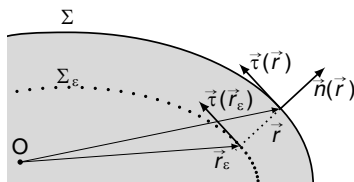


Figure 2. The positional relationship Σ_{ε} and Σ .

if we perform the integration under the limit sign keeping ε to be finite, the obtained expression will have a definite limit at $\varepsilon \rightarrow 0$. The integration in such a manner of strongly singular functions corresponds to the integration in the sense of Hadamard regularization [22].

3. NUMERICAL SOLUTION

The integral Equation (6) is an eigen-value/eigen-function problem. The main idea of the numerical analysis of (6) is based on the discretization of the integral which reduces (6) to a system of linear algebraic equations (SLAE). To reduce the number of numerical calculations it is expedient to use the azimuthal periodicity of the cross-section of the coaxial gyrotron cavity, which leads to the quasi-periodicity of the unknown function $\psi(P_{\alpha_j}\vec{r}) = e^{im\alpha_j}\psi(\vec{r})$, where m is the azimuthal index of the mode, P_{α_j} is the operator of rotation by the angle of $\alpha_j = 2\pi j/N$ in the azimuthal direction, N is the number of corrugations, and $j = 0, 1, 2, \dots, N - 1$. Divide the contour Σ by the contours of periodicity L_j , so $\Sigma = \bigcup_{j=0}^{N-1} L_j$, $P_{\alpha_j}\vec{r} \in L_j$. Then the integral in (6) can be rearranged to

$$\int_{\Sigma} F_{\varepsilon}(\vec{r}, \vec{r}')\psi(\vec{r}') dl' = \int_{L_0} \sum_{j=0}^{N-1} e^{im\alpha_j} F_{\varepsilon}(\vec{r}, P_{\alpha_j}\vec{r}') \psi(\vec{r}') dl',$$

where $F_{\varepsilon}(\vec{r}, \vec{r}') = \frac{\partial}{\partial n(\vec{r}_{\varepsilon})} \frac{\partial}{\partial n(\vec{r}')} Y_0(k_{\perp}|\vec{r}_{\varepsilon} - \vec{r}'|)$.

It is obvious that $F_{\varepsilon}(\vec{r}, P_{\alpha_j}\vec{r}') = F_{\varepsilon}(P_{-\alpha_j}\vec{r}, \vec{r}')$. Finally, (6) is reduced to the strongly singular integral equation over the contour of periodicity:

$$\int_L^* G(\vec{r}, \vec{r}')\psi(\vec{r}') dl' = 0, \quad \vec{r} \in L,$$

where $G(\vec{r}, \vec{r}') = \sum_{j=0}^{N-1} e^{im\alpha_j} F(P_{-\alpha_j}\vec{r}, \vec{r}')$, and the index zero is omitted.

“*” means that integration should be understood in the following sense

$$\int_L^* G(\vec{r}, \vec{r}')\psi(\vec{r}') dl' = \lim_{\varepsilon \rightarrow 0} \int_L G_{\varepsilon}(\vec{r}, \vec{r}')\psi(\vec{r}') dl', \tag{7}$$

where $G_{\varepsilon}(\vec{r}, \vec{r}') = \sum_{j=0}^{N-1} e^{im\alpha_j} F_{\varepsilon}(P_{-\alpha_j}\vec{r}, \vec{r}')$. Performing parameterization of the contour L : $\vec{r}' = \vec{\varphi}(s)$, $\vec{r} = \vec{\varphi}(t)$, where $s, t \in (a, b)$, we

come to the equation

$$\int_a^{b^*} K(t, s)g(s)\varphi'(s) ds = 0, \tag{8}$$

where $K(t, s) = G(\vec{\varphi}(t), \vec{\varphi}(s))$, $\varphi'(s) = |\vec{\varphi}'(s)|$, $g(s) = \psi(\vec{\varphi}(s))$.

The specific form of $\vec{\varphi}(t)$ depends on the shape of the contour L . Above, for simplicity, we assume that L is a simply connected contour. The generalization to more complex contours can be made elementary. It should be noted that in the case of the coaxial gyrotron cavity L is doubly connected contour (see, Fig. 3).

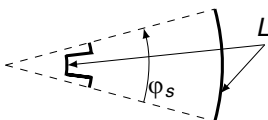


Figure 3. The contour of periodicity of the coaxial gyrotron cavity with a corrugated inner conductor.

To make a discretization, we choose two sets of points on the interval (a, b) :

$$s_i = a + i \frac{(b - a)}{n}, \quad i = 0, 1, \dots, n;$$

$$t_k = \frac{s_{k-1} + s_k}{2}, \quad k = 1, 2, \dots, n.$$

On the internal intervals (s_{i-1}, s_i) , $i = 2, \dots, n - 1$, we approximate the unknown function $g(s)$ by the interpolational Lagrange polynomials of the second order:

$$g(s) \approx g(t_{i-1}) \frac{(s - t_i)(s - t_{i+1})}{(t_{i-1} - t_i)(t_{i-1} - t_{i+1})} + g(t_i) \frac{(s - t_{i-1})(s - t_{i+1})}{(t_i - t_{i-1})(t_i - t_{i+1})} + g(t_{i+1}) \frac{(s - t_{i-1})(s - t_i)}{(t_{i+1} - t_{i-1})(t_{i+1} - t_i)}. \tag{9}$$

On the first (s_0, s_1) and the last (s_{n-1}, s_n) intervals, we approximate $g(s)$ by the interpolational Lagrange polynomials of the first order:

$$g(s) \approx g(t_1) \frac{(s - t_2)}{(t_1 - t_2)} + g(t_2) \frac{(s - t_1)}{(t_2 - t_1)},$$

$$g(s) \approx g(t_{n-1}) \frac{(s - t_n)}{(t_{n-1} - t_n)} + g(t_n) \frac{(s - t_{n-1})}{(t_n - t_{n-1})}. \tag{10}$$

After the substitution of (9) and (10) into (8) we should make an integration. Then, in the obtained relation, we can put $t = t_k$, and come to the SLAE

$$\sum_{i=1}^n M_{ki}(k_{\perp})g(t_i) = 0, \quad k = 1, \dots, n. \quad (11)$$

The details of this procedure can be found in Appendix A.

The non-trivial solution of (11) exists if $\det \|M_{ki}(k_{\perp})\| = 0$, which yields the dispersion equation to define the transverse wavenumbers (eigenvalues) of the eigen-modes. Then, using (11) and (5), we can find the membrane functions everywhere in the cross-section of the coaxial gyrotron cavity.

4. NUMERICAL RESULTS

4.1. Inspection of Results Concerning the Eigenvalues and Ohmic Losses Calculations for the Idealized Geometry of Corrugations

The approach developed allows us to analyze the gyrotron cavities with an arbitrary form of the cross-section, and in particular to analyze a coaxial gyrotron cavity with an inner conductor having an arbitrary form of corrugations. Of interest is to inspect the results obtained previously for an idealized geometry of corrugations. In particular, it would be expedient to verify the results for ohmic losses, which are based on the singular integral equation (SIE) method [14] and the space harmonic method (SHM) [12, 13]. Both of them provide almost identical results for ohmic losses that are rather different from those based on SIM [3]. They rigorously take into account the geometry of corrugations, but at the same time they essentially use geometrical idealizations. The question arises whether these notable differences are caused by geometrical idealizations. It should be pointed out that SIM doesn't correctly take into account the geometry of corrugations, requiring only that the averaged boundary conditions be satisfied.

The numerical calculations were accomplished for the entrance and the middle cross-sections of the $TE_{34,19}$ gyrotron cavity and were compared to the SIE results. In the middle cross-section $f(z)$ and ohmic losses are maximal. The parameters of the middle cross-section are: $R_0 = 29.55$ mm, $R_i = 7.86$ mm, $L = R_i\varphi_L = 0.35$ mm, $d = 0.44$ mm, $N = 75$. At the entrance cross-section ($R_0 = 28.397$ mm, $R_i = 8.384$ mm, other parameters are the same) $f(z)$ and, consequently, ohmic losses are much smaller and, therefore, were not calculated.

The results of the calculations of the averaged density of ohmic losses and normalized eigenvalues for rectangular and wedged grooves at different rounding radii r_0 for the operational $TE_{34,19}$ mode are summarized in Table 1.

For calculations we used the expression which follows from the energy balance of the coaxial gyrotron cavity

$$\rho = \frac{1}{2\pi R_i} \int_{\Sigma} \overline{(\vec{E} \times \vec{H})}_n dl = \frac{1}{4\pi R_i} \delta k_{\perp}^2 \frac{Q_{\text{diff}} P_{\text{out}}}{\int_0^{z_{\text{out}}} |f(z)|^2 dz} \int_{\Sigma} |\psi|^2 dl,$$

where R_i is the maximal radius of the corrugated inner conductor, the top line means the averaging over the oscillation period, Q_{diff} is the diffractive quality factor, P_{out} is the output power, $\delta = \sqrt{\frac{2}{\sigma\omega\mu_0}}$ is the skin depth, μ_0 is the vacuum magnetic permeability, and z_{out} is the length of the coaxial gyrotron cavity. We also assumed that $P_{\text{out}} = 2.2 \text{ MW}$, $Q_{\text{diff}} = 1662$, and $\sigma = 1.4 \cdot 10^7 \text{ S/m}$ is the conductivity of the wall material. It should be pointed out that for the case considered $\delta \approx 3.26 \cdot 10^{-4} \text{ mm}$.

Table 1. Dependencies of eigenvalues and ohmic losses on the rounding radius r_0 .

$r_0, \text{ mm}$	Rectangular grooves with rounded edges		Wedged grooves with rounded edges		SIE, wedged grooves with sharp edges	
	$\chi = R_0 k_{\perp}$	$\rho, \text{ kw/cm}^2$	χ	ρ	χ	ρ
Middle cross-section						
0	105.1942	-	105.1942	0.0308	105.1942	0.0308
10^{-3}	105.1942	0.0291	105.1942	0.0307	-	-
10^{-2}	105.1942	0.0289	105.1942	0.0305	-	-
0.025	105.1943	0.0288	105.1943	0.0305	-	-
0.05	105.1944	0.0292	105.1944	0.031	-	-
0.08	105.1946	0.0306	105.1946	0.0322	-	-
Entrance cross-section						
0	105.2314	-	105.2324	-	105.2325	-
10^{-3}	105.2314	-	105.2324	-	-	-
10^{-2}	105.2319	-	105.2328	-	-	-
0.025	105.2331	-	105.2339	-	-	-
0.05	105.2358	-	105.2367	-	-	-
0.08	105.2400	-	105.2409	-	-	-

Point out that in the expression for ρ the contribution of the transverse magnetic field \vec{H}_\perp has been neglected. Rough estimations for the rounded corrugations and SIE numerical calculations for $r_0 = 0$ show that in the middle cross-section it is inessential.

According to the results obtained, the averaged density of ohmic losses for both wedged grooves with rounded edges and rectangular grooves with rounded edges agree well with the SIE results for the idealized geometry (within an accuracy of 5%) for rounding radii inside the interval 0.001–0.08 mm. Moreover, in the case of rectangular grooves with a rounding radius of about 0.025 mm, the losses were minimal. For larger rounding radii (0.08–0.1 mm), losses somewhat increased. At both cross-sections, the eigenvalues only slightly depend on the rounding radius. Taking into account that the field distribution at the entrance cross-section is the most sensitive to the inner insert, one can conclude that the eigenvalues depend negligibly on the rounding radius all inside the gyrotron cavity. Such a dependence does not lead to a recognizable change of the resonant frequency and the quality factor of the operational mode.

Also, it was found that only the field in the vicinity of the rounding is sensitive to the value of the rounding radius (see Fig. 4. Here and in Fig. 6 all snapshots have the same normalization).

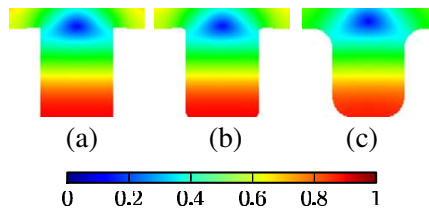


Figure 4. Distribution of $|H_z|$ inside and near the groove of the rectangular shape (arbitrary units): (a) $r_0 = 0.01$ mm, (b) $r_0 = 0.025$ mm, (c) $r_0 = 0.1$ mm.

We can see that the field on the bottom of the grooves is maximal, providing a significant contribution to the total ohmic losses (about 50%), regardless of rounding radius. It was also found earlier on the basis of other approaches [12, 15]. For the wedged groove the distribution of $|H_z|$ is very similar and also slightly depends on the rounding radius.

4.2. Investigation of Influence of Shape of Corrugations on Eigenvalues and Ohmic Losses in the Inner Conductor. The Possibility of Decrease of the Ohmic Losses in the Inner Conductor

Having such a universal technique, it would be interesting to investigate the influence of the groove shape on the ohmic losses in the inner conductor. However, a complete and detailed investigation of this issue is rather extensive and can be a subject of a separate publication. Here, we consider only the special case in which a decrease of ohmic losses can be provided. From the comparative analysis of the results for wedged and rectangular grooves, we can see that rectangular grooves provide slightly lower losses than wedged ones. So, probably, grooves with the width increasing towards the bottom (see, Fig. 5) can provide a further decrease in ohmic losses.

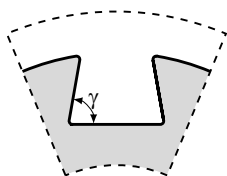


Figure 5. Grooves with the width increasing towards the bottom.

In this case, the shape of the grooves can be defined by the angle γ . Results for ρ and χ at different γ and $r_0 = 0.01$ mm are presented in Table 2. Other parameters are the same as in Table 1.

Table 2. Dependence of losses and eigenvalues on γ .

γ , rad	Middle cross-section		Entrance cross-section
	χ	ρ , kw/cm ²	χ
1.593	105.1943	0.0306	105.2330
1.539	105.1941	0.0269	105.2305
1.481	105.1940	0.024	105.2284
1.413	105.1939	0.0215	105.2264
1.344	105.1939	0.0196	105.2247
1.276	105.1938	0.0182	105.2232

Thus, using grooves with the width, increasing to the bottom, one can make ohmic losses in the corrugated insert notably lower, keeping the eigenvalue almost the same. According to the calculations of the field distribution inside and near the groove illustrated in Fig. 6

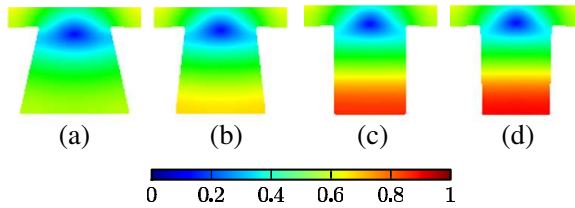


Figure 6. Distribution of $|H_z|$ inside and near the groove with the width increasing towards the bottom (arbitrary units): (a) $\gamma = 1.35$ rad, (b) $\gamma = 1.46$ rad, (c) $\gamma = 90^\circ$ (rectangular grooves), (d) wedged grooves.

the field that penetrates to the bottom of grooves is substantially weaker. Most likely, it can be connected with more intensive and numerous reflections of the field inside the groove and with the increased volume of the groove. As a result, due to self-interference the field distributes inside the increased volume of the groove more homogeneously, decreasing at the boundary of the groove. It should be pointed out that in the case of $\gamma < 1.35$, the narrowest depth of the corrugation is less than 0.1 mm. It can cause problems with the fabrication and exploitation of such components. They can not be manufactured directly. Only manufacturing via electroplating would be possible, while some technical problems also occur. However, the main goal of the example considered to show the possibility of reduction of losses due to a proper choice of the corrugation shape. The practical optimization can be continued further, compromising all technical requirements.

5. CONCLUSION

The rigorous mathematical technique for the analysis of the coaxial gyrotron cavity with an arbitrarily corrugated insert has been demonstrated. In the current straightforward variant of numerical analysis, we use the idea of the direct discretization of the strongly singular integral equation [18, 19]. In the case at hand, the strong singularity in the kernel increases the conditionality of the problem and stability of the numerical calculations. In this regard, the approach developed can be a reasonable alternative to the more traditional consideration based on (5), which can be reduced to the second kind Fredholm integral equation [23]. After the discretization we have SLAE with the diagonal dominance, since the kernel grows rapidly at $\vec{r}' \rightarrow \vec{r}$. Due to this, it provides the same convergence and stability

of numerical results as the second kind Fredholm integral equation. Such an approach can be especially useful in the problems when the strong singularity can not be avoided (for example, waveguides with anisotropic media or more complex boundary conditions and so forth), and the traditional regularization is associated with significant analytical or numerical difficulties.

The developed technique allows us to consider in detail at least two important aspects. Both of them have concern not only to coaxial gyrotron cavities but also can be interesting for other microwave devices and even more widely for microwave engineering.

First, many microwave devices include components that have almost sharp metallic edges. Very often, for simplicity, the idealized geometry is considered, which neglects the small natural rounding near the sharp edges. Such an idealization provokes the appearance of an integrable singularity in field components. The macroscopic consequences of such an idealization are often not clearly understood. Indeed, the idealized perfectly conducting boundary condition $E_\tau = 0$ (which here is expressed by (3)) is the limiting case of the impedance boundary conditions. In turn, the impedance boundary conditions are rigorously valid only in the case of $r_0 \gg \delta$, where r_0 is the radius of a surface curvature. So, near the sharp edge ($r_0 = 0$), the ideal and even impedance boundary conditions are not correct. Therefore, the feasibility of such an idealization in many practical cases is an open question and should be inspected. Some qualitative discussion on this issue however without any calculational confirmation can be found in [24].

For the case at hand, the geometrical idealizations assumed earlier in calculations of ohmic losses by full wave approaches [11, 12] are entirely reasonable. They do not influence results and can not be the reasons for the discrepancy between the theoretical predictions and the experimental measurements of the ohmic losses in the inner conductor revealed in [16] for the $TE_{31,17}$ coaxial gyrotron cavity.

Second, ohmic losses in the walls of resonators is the general problem of vacuum high-power microwave sources and particle accelerators. Therefore finding methods of decreasing ohmic losses is of general interest. In particular, a remarkable decrease of ohmic losses in the corrugated inner conductor of the coaxial gyrotron cavity was revealed earlier for the wedged grooves with sharp edges [15]. It can be achieved by the proper choice of the depth of grooves. However, this method can hardly be used to improve the ITER relevant coaxial gyrotrons, since the depth of the grooves should be kept inside the interval $0.2 < d/\lambda_c < 0.25$, where λ_c is the cutoff wavelength of the operational mode, to avoid self-excitation on the higher cyclotron

harmonics [3, 5].

Results obtained here show that another way in which the remarkable decreasing the ohmic losses is also possible. It can be based on a proper choice of the corrugation shape. One type of shape that yields reduced ohmic losses has been demonstrated. Namely, corrugations with the width increasing towards the bottom provide substantially lower ohmic losses compared to the rectangular corrugations currently used in coaxial gyrotron cavities.

At the same time, it is shown that the eigenvalues of the eigenmodes and, consequently, the resonant frequencies and quality factors are not sensitive to the shape of corrugations. So, specific mode selection properties of the coaxial gyrotron cavity are conserved at such changes of the shape of the grooves. So, this fact can be utilized for decreasing ohmic losses in the inner conductor and can be, in practice, exploited for the optimization of the coaxial gyrotron cavities.

Concerning the basic physics of this effect one should be mentioned that, in accordance with the field distribution inside corrugations (see Fig. 6), such a form of corrugations prevents the penetration of the field to the bottom of the grooves due to numerous reflections and self-interference inside the grooves. Also due to these effects the field distributes more uniformly inside the increased volume of the groove. Therefore, the substantial decrease of the field at the groove walls is achieved. For the case at hand, ohmic losses in the corrugated inner conductor can be even lower than those in the case of the smooth inner conductor.

The obtained results can be useful for sophistication of mathematical description of resonators in high-power microwave sources and improvement of their performance.

ACKNOWLEDGMENT

Authors are grateful to Prof. V. A. Scherbina from the Department of Mathematical Physics and Computational Mathematics, Karazin Kharkov National University, Ukraine, for important comments, and to Dr. S. Kern and Prof. M. Thumm from the Institute of Pulsed Power and Microwave Technology, Karlsruhe Institute of Technology for valuable discussions.

APPENDIX A.

After the interpolation of the unknown function $g(s)$ by the Lagrange polynomials (see (9), (10)) and inserting it into (8) in order to find the

matrix coefficients $M_{ki}(k_{\perp})$, we should calculate the integrals of the kind

$$I_k^p = \int_a^{b^*} K(t_k, s) s^p \varphi'(s) ds = \lim_{\varepsilon \rightarrow 0} \int_a^b K_{\varepsilon}(t_k, s) s^p \varphi'(s) ds \quad (A1)$$

for $p = 0, 1, 2$. Here we denote

$$K_{\varepsilon}(t, s) = G_{\varepsilon}(\vec{r}(t), \vec{r}'(s)) = G(\vec{\varphi}(t) - \varepsilon \vec{n}(t), \vec{\varphi}(s)), \quad \vec{n}(t) = \vec{n}(\vec{\varphi}(t)).$$

The direct numerical integration of (A1) is impossible, since the integral becomes divergent at $\varepsilon \rightarrow 0$. In order to circumvent this we should extract the singular part from the kernel in such a way which allows us to evaluate the relevant singular integral analytically and then take the limit of $\varepsilon \rightarrow 0$. The regular part of the integral is discretized directly. For the sake of convenience, we perform the extracting in two steps.

First, using the asymptotic of the Neumann function at small arguments and $\frac{\partial}{\partial n(\vec{r})} = (\vec{n}(\vec{r}), \frac{\partial}{\partial \vec{r}})$, we represent $G_{\varepsilon}(\vec{r}, \vec{r}')$ as a sum of two parts. One of them remains regular and another becomes singular at $\vec{r} = \vec{r}'$, $\varepsilon \rightarrow 0$:

$$G_{\varepsilon}(\vec{r}, \vec{r}') = G_{1\varepsilon}(\vec{r}, \vec{r}') + G_{2\varepsilon}(\vec{r}, \vec{r}'), \quad (A2)$$

where

$$G_{1\varepsilon}(\vec{r}, \vec{r}') = \frac{2}{\pi} \frac{\partial^2}{\partial n(\vec{r}_{\varepsilon}) \partial n(\vec{r}')} \ln k_{\perp} R_{\varepsilon} - \frac{1}{\pi} (\vec{n}(\vec{r}_{\varepsilon}), \vec{n}(\vec{r}')) \ln k_{\perp} R_{\varepsilon}$$

is singular, and $G_{2\varepsilon}(\vec{r}, \vec{r}')$ is some regular function. Here we denote $R_{\varepsilon} = |\vec{r}_{\varepsilon} - \vec{r}'|$. It should be noted that the singularity can appear only in the term of the sum with $j = 0$. Respectively, $K_{\varepsilon}(t, s) = K_{1\varepsilon}(t, s) + K_{2\varepsilon}(t, s)$, where $K_{1,2\varepsilon}(t, s) = G_{1,2\varepsilon}(\vec{\varphi}(t), \vec{\varphi}(s))$.

Second, using the identity [18]

$$\frac{\partial^2}{\partial n(\vec{r}_{\varepsilon}) \partial n(\vec{r}')} = - \frac{\partial^2}{\partial \tau(\vec{r}_{\varepsilon}) \partial \tau(\vec{r}')},$$

where $\vec{\tau}(\vec{r}_{\varepsilon}) = \vec{\tau}(\vec{r}) = \vec{\varphi}'(t)/\varphi'(t)$ is the unit tangent vector to the contour in the point \vec{r}_{ε} (see, Fig. 2), and $\vec{r}' \approx \vec{\varphi}(t) + \vec{\varphi}'(t)(s - t) + \frac{Q}{2}(s - t)^2$ at $s \rightarrow t$, $K_{1\varepsilon}(t, s)$ can be presented as $K_{1\varepsilon}(t, s) = K_{S\varepsilon}(t, s) + K_{R\varepsilon}(t, s)$, where

$$K_{S\varepsilon}(t, s) = - \frac{2}{\pi} \frac{1}{\varphi'(t)} \frac{\partial}{\partial t} \left(\frac{1}{\varphi'(s)} \frac{\partial}{\partial s} \ln(k_{\perp} |\vec{\varphi}'(t)(s - t) - \varepsilon \vec{n}(t)|) \right) - \frac{1}{\pi} \frac{\varphi'(t)}{\varphi'(s)} \ln(k_{\perp} |\vec{\varphi}'(t)(s - t) - \varepsilon \vec{n}(t)|),$$

$K_{R\varepsilon}(t, s)$ is the regular function. Since $\vec{n}(t) \perp \vec{\varphi}'(t)$, we have $|\vec{\varphi}'(t)(s - t) - \varepsilon\vec{n}(t)| = \sqrt{\varphi'^2(t)(s - t)^2 + \varepsilon^2}$. $K_{S\varepsilon}(t, s)$ is singular at $s \rightarrow t, \varepsilon \rightarrow 0$. However, integration of $K_{S\varepsilon}(t_k, s)$ can be performed analytically at a finite ε :

$$\int_a^b K_{S\varepsilon}(t, s) s^p \varphi'(s) ds = -\frac{1}{\pi \varphi'(t)} \frac{d}{dt} J_1^p(t) - \frac{1}{2\pi} \varphi'(t) J_2^p(t),$$

where

$$\begin{aligned} J_1^p(t) &= \int_a^b s^p \frac{\partial}{\partial s} \ln \left(k_{\perp} (\varphi'^2(t)(s - t)^2 + \varepsilon^2) \right) ds \\ &= s^p \ln \left(k_{\perp} (\varphi'^2(t)(s - t)^2 + \varepsilon^2) \right) \Big|_a^b - (\delta_{1p} + \delta_{2p}) p I_2^{p-1}(t), \\ J_2^p(t) &= \int_a^b s^p \ln \left(k_{\perp} (\varphi'^2(t)(s - t)^2 + \varepsilon^2) \right) ds, \end{aligned}$$

δ_{ik} is the Kronecker delta. The last integral is the table integral [25] and exists also at $\varepsilon = 0$.

Now, putting in $I_{1,2}^p(t)$, $K_{R\varepsilon}(t, s)$ and $K_{2\varepsilon}(t, s)$ $t = t_k$ and $\varepsilon = 0$, we have

$$\begin{aligned} I_k^p &= -\frac{1}{\pi} \left(\frac{2}{\varphi'(t)} \frac{d}{dt} J_1^p(t) + \frac{1}{\pi} \varphi'(t) J_2^p(t) \right) \Big|_{t=t_k, \varepsilon=0} \\ &\quad + \int_a^b (K_R(t_k, s) + K_2(t_k, s)) s^p \varphi'(s) ds, \end{aligned} \tag{A3}$$

where $K_{R,2}(t, s) = \lim_{\varepsilon \rightarrow 0} K_{R\varepsilon,2\varepsilon}(t, s)$.

Integration of the last term in (A3) can be performed using interpolation formulas like (9) and (10) or any standard methods of numerical integration.

REFERENCES

1. Rzesnicki, T., B. Piosczyk, S. Kern, et al., "2.2-MW record power of the 170-GHz European preprototype coaxial-cavity gyrotron for ITER," *IEEE Trans. Plasma Sci.*, Vol. 38, No. 6, 1141–1149, Jun. 2010.

2. Zapevalov, V. E., V. I. Khizhnyak, M. A. Moiseev, A. B. Pavelyev, and N. I. Zavolsky, "Advantages of coaxial cavity gyrotrons," *Proceedings of the 12th Joint Workshop 'Electron Cyclotron Emission and Electron Cyclotron Heating'*, 423–432, Aix-en-Provence, France, May 13–16, 2002.
3. Iatrou, C. T., S. Kern, and A. B. Pavelyev, "Coaxial cavities with corrugated inner conductor for gyrotrons," *IEEE Trans. Microwave Theory Tech.*, Vol. 44, 56–64, Jan. 1996.
4. Iatrou, C. T., "Mode selective properties of coaxial gyrotron resonators," *IEEE Trans. Plasma Sci.*, Vol. 24, No. 3, 596–605, Jun. 1996.
5. Avramides, K., C. Iatrou, and J. Vomvoridis, "Design considerations for powerful continuous-wave second-cyclotron-harmonic coaxial-cavity gyrotrons," *IEEE Trans. Plasma Sci.*, Vol. 32, No. 3, 917–928, 2004.
6. Dumbrajs, O., K. A. Avramides, and B. Piosczyk, "Mode competition in the 170 GHz coaxial gyrotron cavity for ITER," *Proc. of Joint 32nd Int. Conf. IRMMW-THz.*, 48–49, 2007.
7. Barroso, J. J., R. A. Correa, and P. J. Castro, "Gyrotron coaxial cylindrical resonators with corrugated inner conductor: Theory and experiment," *IEEE Trans. Microwave Theory Tech.*, Vol. 46, No. 9, 1221–1230, Sep. 1998.
8. Singh, K., P. Jain, and B. Basu, "Analysis of a coaxial waveguide corrugated with wedge-shaped radial vanes considering azimuthal harmonic effects," *Progress In Electromagnetics Research*, Vol. 47, 297–312, 2004.
9. Piosczyk, B., G. Dammertz, O. Dumbrajs, et al., "A 2 MW, 170 GHz coaxial cavity gyrotron — Experimental verification of the design of main components," *Journal of Physics: Conference Series*, Vol. 25, 24–32, 2005.
10. Grundiev. A., J.-Y. Raguin, and K. Schunemann, "Numerical study of mode competition in coaxial gyrotrons with corrugated insert," *International Journal of Infrared and Millimeter Waves*, Vol. 24, No. 2, Feb. 2003.
11. Gandel, Y. V., G. I. Zaginaylov, and S. A. Steshenko, "Rigorous electromagnetic analysis of coaxial gyrotron cavities," *Technical Physics*, Vol. 49, 887–894, 2004.
12. Ioannidis, Z. C., O. Dumbrajs, and I. O. Tigelis, "Eigenvalues and Ohmic losses in coaxial gyrotron cavity," *IEEE Trans. Plasma Sci.*, Vol. 34, No. 4, 1516–1522, 2006.
13. Ioannidis, Z. C., K. A. Avramides, G. P. Latsas, and I. G. Tigelis,

- “Azimuthal mode coupling in coaxial waveguides and cavities with longitudinally corrugated insert,” *IEEE Trans. Plasma Sci.*, Vol. 39, No. 5, 1213–1221, 2011.
14. Dumbrajs, O. and G. I. Zaginaylov, “Ohmic losses in coaxial gyrotron cavity with corrugated insert,” *IEEE Trans. Plasma Sci.*, Vol. 32, 861–866, Jun. 2004.
 15. Zaginaylov, G. I., N. N. Tkachuk, V. I. Shcherbinin, and K. Schuenemann, “Rigorous calculation of energy losses in cavity of ITER relevant coaxial gyrotron,” *Proceedings of 35th European Microwave Conference*, 1107–1110, Paris, France, 2005.
 16. Piosczyk, B., et al., “165-GHz coaxial cavity gyrotron,” *IEEE Trans. on Plasma Science*, Vol. 32, 853–860, Jun. 2004.
 17. Collin, R. E., *Field Theory of Guided Waves*, IEEE Press, New York, 1991.
 18. Shcherbina, V. A., “The diffraction problem in periodic solutions,” *Telecommunication and Radio Engineering*, Vol. 61, No. 5, 382–393, 2004.
 19. Mitina, I. V., “Method of numerical analysis of spectrum of flat resonators,” *Electromagnetic Phenomena*, Vol. 5, No. 1, 26–31, 2005 (in Russian).
 20. Fliflet, A. W., “Linear and non-linear theory of the Doppler-shifted cyclotron resonance maser based on TE and TM waveguide modes,” *Int. J. Electronics*, Vol. 61, No. 6, 1049–1080, 1986.
 21. Katsenelenbaum, B. Z., L. Mercader del Rio, M. Pereyaslavets, M. Sorolla Ayza, and M. Thumm, *Theory of Nonuniform Waveguides: The Cross-section Method*, The Institution of Electrical Engineers, London, 1998.
 22. Hadamard, J., *Le Problème de Cauchy et Les Équations Aux Dérivées Partielles Linéaires Hyperboliques*, Hermann & Cie., Paris, 1932 (in French).
 23. Galishnikova, T. N. and A. S. Il’insky, *Numerical Methods in the Diffraction Problems*, Edition of Moscow University, 1987 (in Russian).
 24. Il’insky, A. S., A. Ja Slepjan, and G. Ja Slepjan, *Propagation, Diffraction and Dissipation of Electromagnetic Waves*, The IEE and Peter Peregrinus Ltd. *Electromagnetic Waves*, Series 36, London, UK, 1993.
 25. Gradshteyn, I. S. and I. M. Ryzhik, *Table of Integrals, Series and Products*, 7th edition, A. Jeffrey and D. Zwillinger (eds.), Academic Press, New York, 2007.